Journal Pre-proofs

Discovery of Thieno[2,3-*d*]pyrimidin-4(3*H*)-one Derivatives as a New Class of ROCK Inhibitors

Zhuang Miao, Yu-meng Sun, Lan-ying Zhao, Yue-shan Li, Yi-fei Wang, Jin-shan Nan, Ze-en Qiao, Lin-li Li, Sheng-yong Yang

PII: S0960-894X(20)30019-6
DOI: https://doi.org/10.1016/j.bmcl.2020.126966
Reference: BMCL 126966

To appear in: *Bioorganic & Medicinal Chemistry Letters*

Received Date: 21 November 2019
Revised Date: 3 January 2020
Accepted Date: 11 January 2020

Please cite this article as: Miao, Z., Sun, Y-m., Zhao, L-y., Li, Y-s., Wang, Y-f., Nan, J-s., Qiao, Z-e., Li, L-l., Yang, S-y., Discovery of Thieno[2,3-*d*]pyrimidin-4(3*H*)-one Derivatives as a New Class of ROCK Inhibitors, *Bioorganic & Medicinal Chemistry Letters* (2020), doi: https://doi.org/10.1016/j.bmcl.2020.126966

Discovery of Thieno[2,3-*d*]pyrimidin-4(3*H*)-one Derivatives as a New Class of ROCK Inhibitors

Zhuang Miao[a,#], Yu-meng Sun[b,#], Lan-ying Zhao[a], Yue-shan Li[a], Yi-fei Wang[b], Jin-shan Nan[a], Ze-en Qiao[a], Lin-li Li[b,*], Sheng-yong Yang[a,*]

[a]*State Key Laboratory of Biotherapy and Cancer Center, West China Hospital, Sichuan University, Chengdu, Sichuan 610041, China.*

[b]*Key Laboratory of Drug Targeting and Drug Delivery System of Ministry of Education, West China School of Pharmacy, Sichuan University, Chengdu, Sichuan 610041, China*

# These authors contributed to this work equally

* Corresponding author. Tel.: +86-28-85164063; fax: +86-28-85164060

E-mail address: (Sheng-yong Yang) yangsy@scu.edu.cn;

(Lin-li Li) ysylilinli@sina.com

Abstract

Herein, we report the discovery of a series of thieno[2,3-*d*]pyrimidin-4(3*H*)-one derivatives as a new class of ROCK inhibitors. Structure-activity relationship studies of these compounds led to the identification of the most potent compound, 3-(3-methoxybenzyl)-6-(1H-pyrrolo[2,3-*b*]pyridin-4-yl)thieno[2,3-*d*]pyrimidin-4(3*H*)-one (**8k**), which showed IC_{50} values of 0.004 μM and 0.001 μM against ROCK I and ROCK II, respectively. *In vitro*, **8k** significantly reduced the phosphorylation level of ROCK downstream signaling protein and induce changes in cell morphology and migration. Overall, this study provides a promising lead compound for drug discovery targeting ROCK.

Keywords

ROCK, kinase inhibitor, structure-activity relationship, cell migration, cell morphology

Rho-associated coiled-coil containing protein kinases (ROCKs) belong to the AGC subfamily of the serine/threonine protein kinases. There are two isoforms for ROCK, namely, ROCK I and ROCK II, which share 65% overall sequence homology and are highly homologous in their ATP-binding pocket.[1] After activated by GTP-bound Rho protein, ROCKs trigger changes in cell morphology[2] and migration[2,3], and regulates cytoskeleton through the phosphorylation of their numerous downstream proteins. Myosin light chain (MLC) and the myosin phosphatase targeting subunit 1 (MYPT1) act as the main substrates of ROCKs, which are highly associated with contractility of smooth muscle cells.[1] Therefore, ROCK inhibition provides a potential treatment where smooth muscle intervention is required, such as erectile dysfunction,[4] glaucoma,[5,6] pulmonary arterial hypertension,[7] and cardiovascular disease.[8,9] In addition, symptoms including neurological disorders,[10] tumorigenesis,[11] and Bullous Keratopathy[12] have also been demonstrated to be linked with ROCKs. Currently, a number of ROCK inhibitors have been reported[13] and three of them (Fasudil, Ripasudil and Netarsudil) have been approved to use clinically (**Figure 1**). Fasudil is prescribed for the treatment of cerebral vasospasm. Ripasudil and Netarsudil are used for the treatment of glaucoma by increasing aqueous humor outflow.[14,15] Even so, discovering more potent ROCK inhibitors with new scaffolds is still necessary, which is for increasing additional options for coping with other indications and possible drug resistance in future.

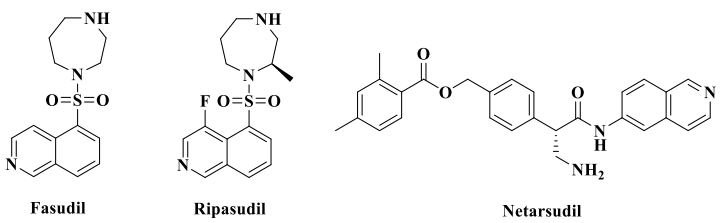

Figure 1. Chemical structures of clinically used ROCK inhibitors.

To achieve this goal, we conducted a molecular docking based virtual screening (VS) against our in-house chemical database (**Figure S1**), which gave a hit compound, 3-(3-methoxybenzyl)-7-(1H-indazol-5-yl)quinazolin-4(3H)-one (**1**, **Figure 2**). This compound displayed moderate inhibitory activity against ROCK (ROCK I: 3.106 μM, and ROCK II: 0.088 μM). We then carried out a structural optimization towards **1** to improve its potency. The structural modifications were focused on three regions, quinazolin-4(3H)-one (region I), indazole (region II), and methoxy benzene (region III). A total of twenty-four compounds (**4a-c**, **8a-l**, **10a-e**, and **11a-e**) were synthesized and the structure-activity relationship was further discussed.

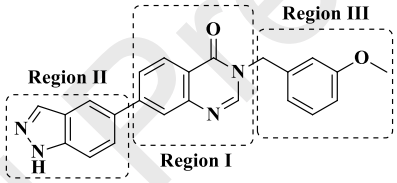

Figure 2. The chemical structure of hit compound **1** obtained by virtual screening.

In the first step, we fixed region II, region III and varied region I. Four compounds (**4a-c**, **8a**) were prepared. **Scheme 1** depicts the synthetic routes of compounds **4a-c**. Briefly, commercially available reagents **2a-c** reacted with 3-methoxybenzyl bromide gave intermediates **3a-c**. Suzuki-Miyaura coupling of **3a-c** with 1*H*-indazole-5-boronic acid pinacol ester generated compounds **4a-c**.

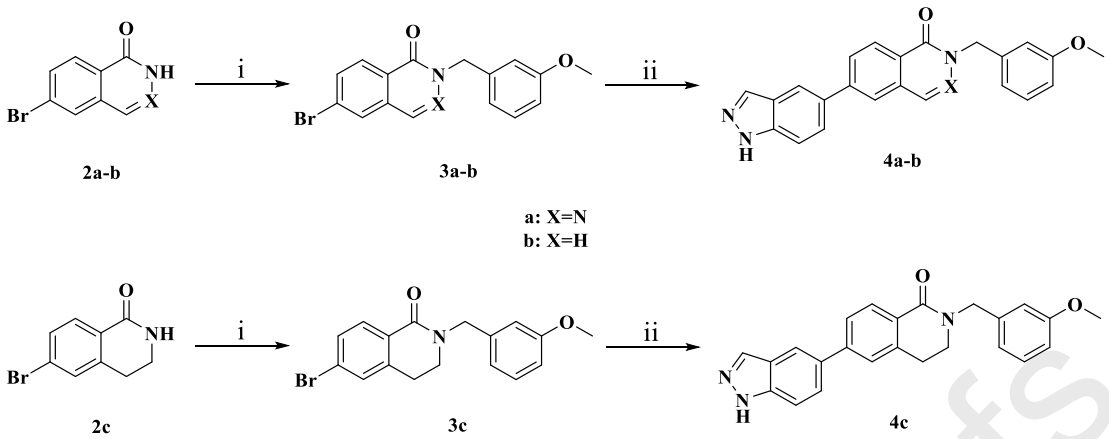

Scheme 1. Synthetic routes of compounds **4a-c**. Reagents and conditions: (i) DMF, 3-methoxybenzyl bromide, NaH, 0 °C – room temperature (RT), 12 h, 35%-45%; (ii) 1,4-dioxane/H_2O (5/1), 1*H*-indazole-5-boronic acid pinacol ester, $Pd(PPh_3)_4$, Cs_2CO_3, N_2, 95 °C, 12 h, 19%-24%.

Chemical structures and ROCK inhibitory activities of these compounds are listed in **Table 1**. Removing N1 or shifting it to 2-position had no obvious enhancement in terms of the potency (**4a**, **4b** vs **1**). A decline in inhibitory activity was observed when isoquinolin-1(2*H*)-one in **4b** was saturated (**4c** vs **4b**). It is worth noting that compound **8a**, which contains a thieno[2,3-*d*]pyrimidin-4(3*H*)-one moiety, showed a significant improvement in ROCK inhibitory potency. Therefore, thieno[2,3-*d*]pyrimidin-4(3*H*)-one was selected as the optimal fragment in region I.

Table 1. Chemical structures and ROCK inhibitory activities of compounds **4a-c** and **8a**.

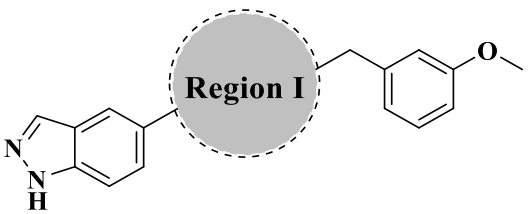

Compound	Region I	IC_{50} (μM)[a]	
		ROCK I	ROCK II
1	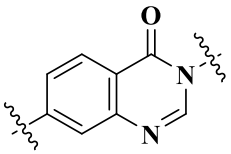	3.106	0.088
4a	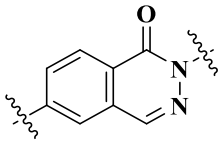	> 10	0.398
4b	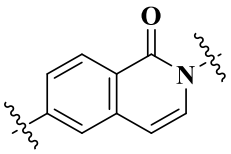	1.877	0.107
4c	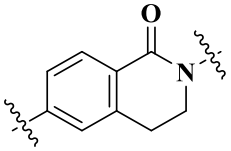	2.062	0.632
8a	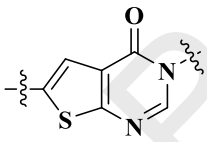	0.020	0.002

[a]IC_{50} values were determined from Kinase Profiler of Eurofins. [ATP] = 10 μM.

In the second step, we optimized region II, with region I fixed as the optimal fragment thieno[2,3-*d*]pyrimidin-4(3*H*)-one and region III fixed as its original group. To this end, various heterocyclic rings were utilized to replace the indazole moiety in region II. A total of 11 new compounds (**8b-l**) were synthesized. **Scheme 2** shows the synthesis routes of compounds **8a-l**. Bromination of thieno[2,3-*d*]pyrimidin-4(3*H*)-one (**5**) under acetic acid produced intermediate **6**. Substitution reaction of intermediate **6** yielded **7**. Then the desired products were obtained through Suzuki-Miyaura coupling of **7** with different boric acid or boric acid ester groups.

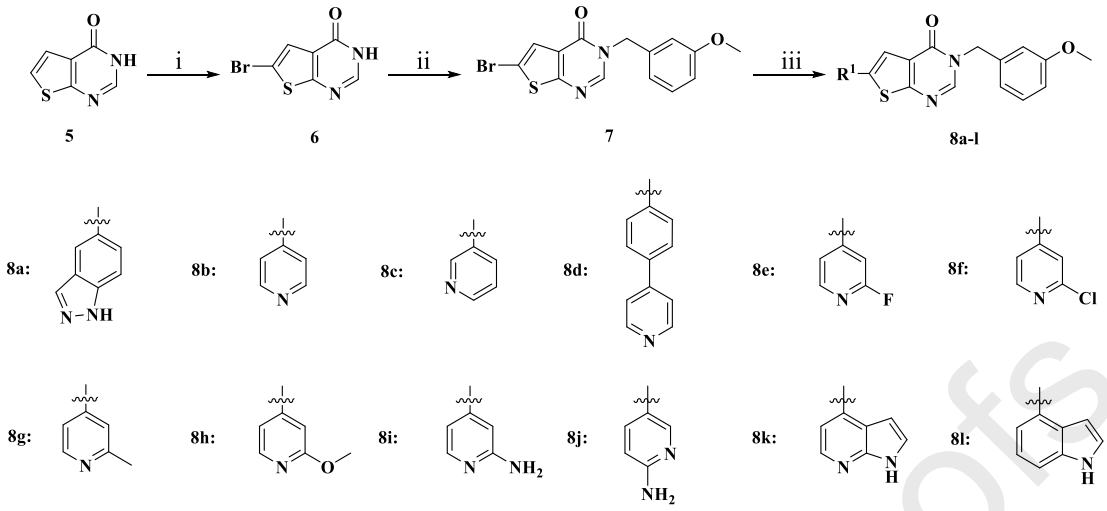

Scheme 2. Synthesis routes of compounds **8a-l**. Reagents and conditions: (i) AcOH, Br_2, RT, 4 h, 90%; (ii) DMF, 3-methoxybenzyl bromide, K_2CO_3, RT, 12 h, 47%; (iii) 1,4-dioxane/H_2O (5/1), $Pd(PPh_3)_4$, Cs_2CO_3 (**8a**) or K_2CO_3 (**8b-l**), N_2, 95 °C, 12 h, 21%-57%.

Table 2 summarizes the chemical structures and ROCK inhibitory activities of these compounds. Compound **8b**, which has a pyridine group, displayed considerable potency against ROCK. Lengthening pyridine by introducing an extra benzene ring, or changing the position of nitrogen atom in pyridine led to an obvious loss in ROCK inhibitory activity (**8c**, **8d** vs **8b**), indicating that the nitrogen atom should be fixed at para-position. We then investigated the possible impact of different substituents on pyridine. The generated compounds all exhibited obviously decreased potencies (**8e-h** vs **8b**) except **8i**, which contains an amino substituent (2-aminopyridine). The inhibitory activity almost disappeared when changing the position of nitrogen atom and the amino group (**8j** vs **8i**). A ring-closed analog (**8k**) of **8i**, which possesses a 7-azaindole fragment, displayed a higher ROCK I activity (IC_{50} = 0.004 μM) and

comparable ROCK II inhibition activity (IC_{50} = 0.001 μM). Replacing azaindole by indole (**8l** vs **8k**) significantly reduced the potency, indicating again the importance of nitrogen atom at para-position. Collectively, 2-aminopyridine or 7-azaindole may be the best choice for region II.

Table 2. Chemical structures and ROCK inhibitory activities of **8b-l**.

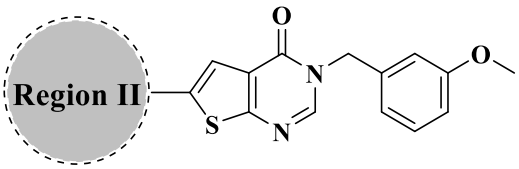

Compound	Region I	IC_{50} (μM)[a]	
		ROCK I	ROCK II
8a	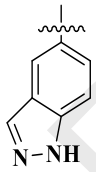	0.020	0.002
8b	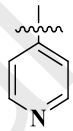	0.045	0.006
8c	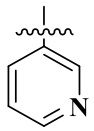	> 10	3.475
8d	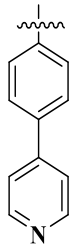	> 10	> 10
8e	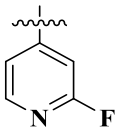	1.050	0.083

8f	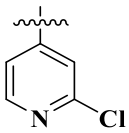	> 10	0.501
8g	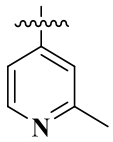	2.515	0.042
8h	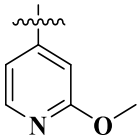	> 10	6.915
8i	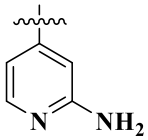	0.018	0.001
8j	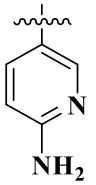	> 10	> 10
8k	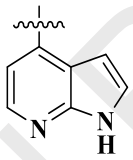	0.004	0.001
8l	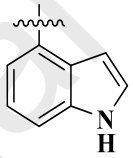	> 10	0.583

[a]IC_{50} values were determined from Kinase Profiler of Eurofins. [ATP] = 10 μM.

In the last step, we optimized region III with region I and II fixed as their optimal groups. A total of ten compounds (**10a-e** and **11a-e**) with different substituted phenyl groups at region III were synthesized. According to the fragments at region II, the prepared compounds were classified into two categories: A (7-azaindole at region II) and B (2-aminopyridine in region II). The synthetic routes for these compounds are given in **Scheme 3**. Substitution reaction of **6** with various substitutional benzyl

bromide afforded intermediates **9a-e**. Suzuki-Miyaura coupling of **9a-e** with 7-azaindole-4-boronic acid pinacol ester or 2-aminopyridine-4-boronic acid pinacol ester provided final compounds **10a-e** or **11a-e**.

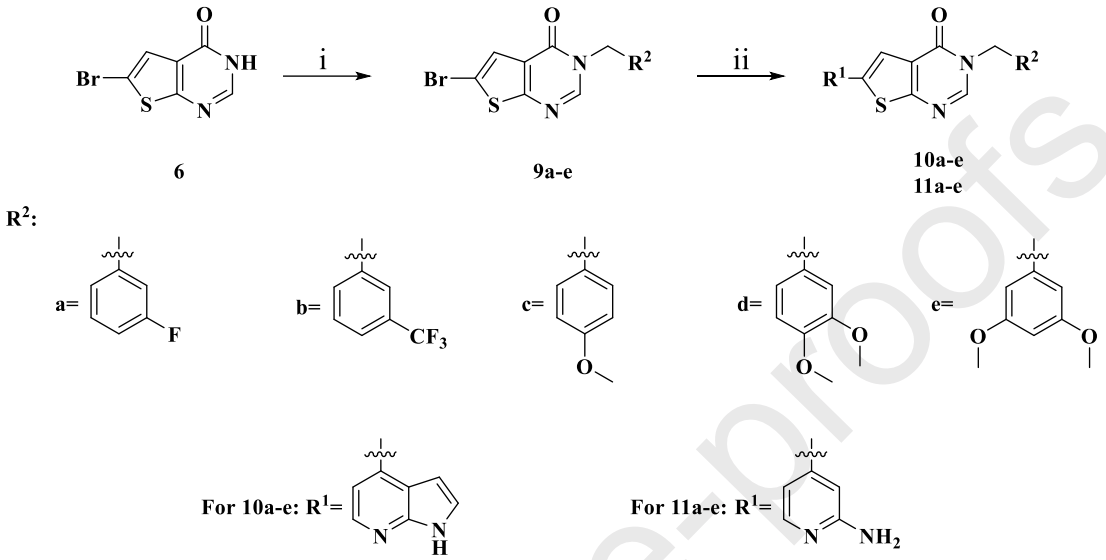

Scheme 3. Synthesis routes of compounds **10a-e** and **11a-e**. Reagents and conditions: (i) DMF, K_2CO_3, RT, 12 h, 41%-53%; (ii) 1,4-dioxane/H_2O (5/1), $Pd(PPh_3)_4$, K_2CO_3, N_2, 95 ^oC, 12 h, 37%-55%.

Chemical structures and ROCK inhibitory activities of these compounds are shown in **Table 3**. It can be seen that compounds **8i** and **8k** are still the best one in their corresponding categories. Therefore, region III was fixed as its original form. Because **8k** was the most potent one among all the synthesized compounds, further studies were carried out only on this compound.

Table 3. Chemical structures and ROCK inhibitory activities of compounds **10a-e** and **11a-e**.

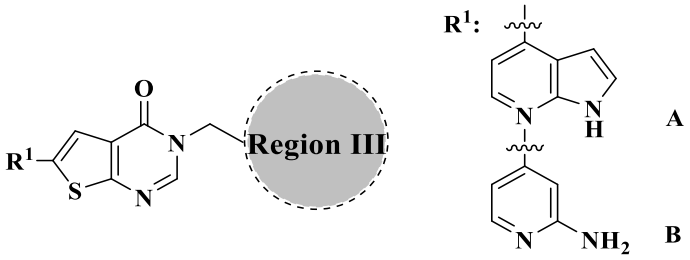

Compound	series	Region III	IC50 (μM)[a]	
			ROCK I	ROCK II
8k	A	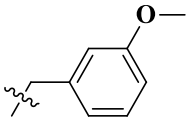	0.004	0.001
10a		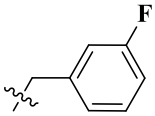	0.013	0.001
10b		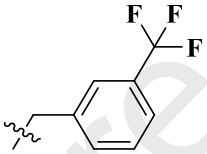	0.110	0.007
10c		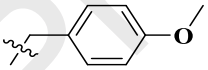	0.013	0.002
10d		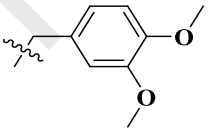	0.025	0.004
10e		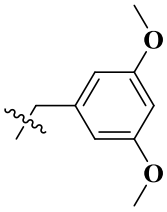	0.074	0.004
8i	B	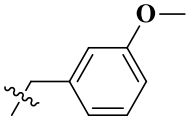	0.018	0.001
11a		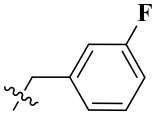	0.034	0.005
11b		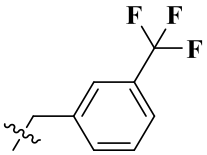	0.490	0.025

11c	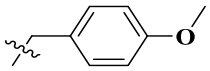	1.445	0.046
11d	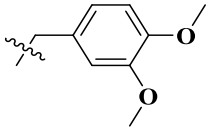	> 10	0.219
11e	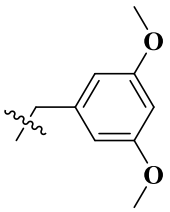	> 10	0.058

[a]IC_{50} values were determined from Kinase Profiler of Eurofins. [ATP] = 10 μM.

Western blot assays were used to examine the activity of compound **8k** in intact cells. Here 293T cells were used, and the phosphorylation level of ROCK direct downstream protein MYPT1 was measured. Phosphatase inhibitor Cocktail was utilized to stabilize phosphorylated MYPT1 (p-MYPT1) because p-MYPT1 is easy to be dephosphorylated at the time of cell disruption. As shown in **Figure 3**, under the protection of Cocktail, we could observe the phosphorylated MYPT1, and **8k** significantly reduced the phosphorylation level of MYPT1. We also noticed that **8k** did not influence the level of MYPT1. Because MYPT1 is one of the common substrates of ROCK I and II [13,16] and **8k** has inhibitory activity against both ROCK I and II, it is expected that the decrease in the phosphorylation level of MYPT1 is due to the co-inhibitory effects of **8k** against ROCK I and ROCK II. Overall, these results demonstrated that **8k** inhibited the ROCK activity in intact cells.

Scratch wound assay was carried out to investigate whether **8k** can induce changes in cell migration. Here, MDA-MB-231 cells were used. As exhibited in **Figure 4**, **8k**

significantly prevented cell migration compared with the control group. We also tracked the cell shape, and observed that most of the MDA-MB-231 cells displayed spindle-shaped morphology on the edges upon **8k** treatment (see **Figure 5**). These results indicate that **8k** is able to inhibit cell migration *in vitro* and has a potential to regulate cell morphology.

Finally, we examined the selectivity of compound **8k**. To this end, 100 representative kinases covering all kinase families were selected. Inhibition rates of **8k** against these kinases were measured at 1 μM (**Table S1**). The human kinome dendrogram based on the measured inhibition rates is shown in **Figure 6**. In addition to ROCKs, **8k** also displays considerable activity against PKA, LIMK2, and Flt1. Of note is that **8k** did not show obvious inhibitory activity against all other tested kinases, indicating a good selectivity. The calculated scores, S(5), S(10) and S(20), are 0.029, 0.049 and 0.137, respectively.

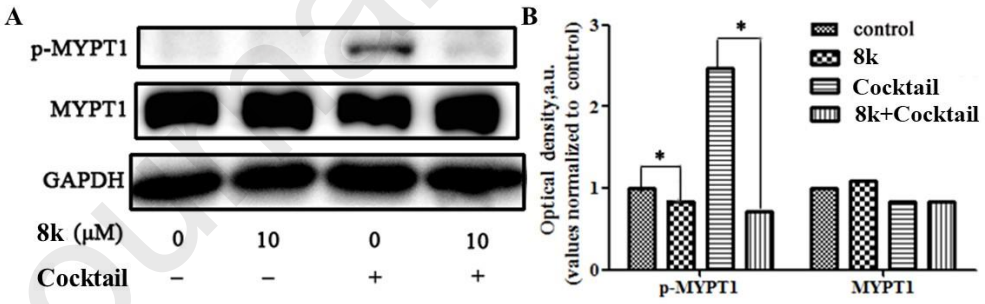

Figure 3. (A) **8k** reduced p-MYPT1 level in the 293T cell line. (B) The quantification of the immunoblot (* $P < 0.05$, t test).

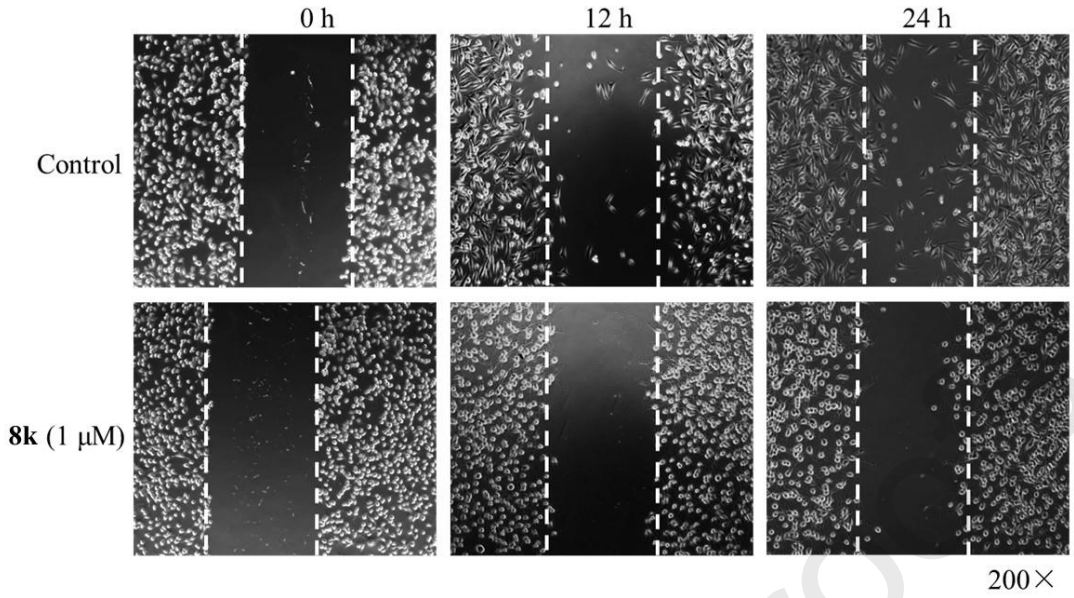

Figure 4. 8k inhibited MDA-MB-231 cells migration *in vitro*.

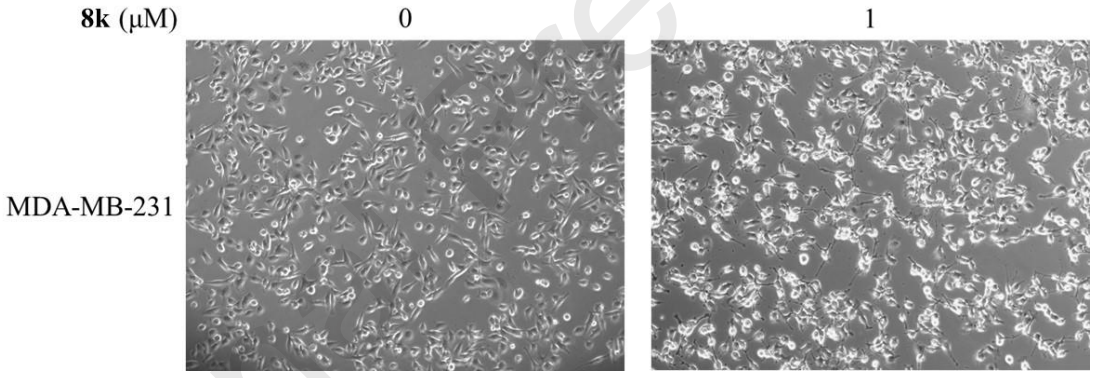

Figure 5. MDA-MB-231 cells morphology changes at 60 min after treating with 1 μM **8k**.

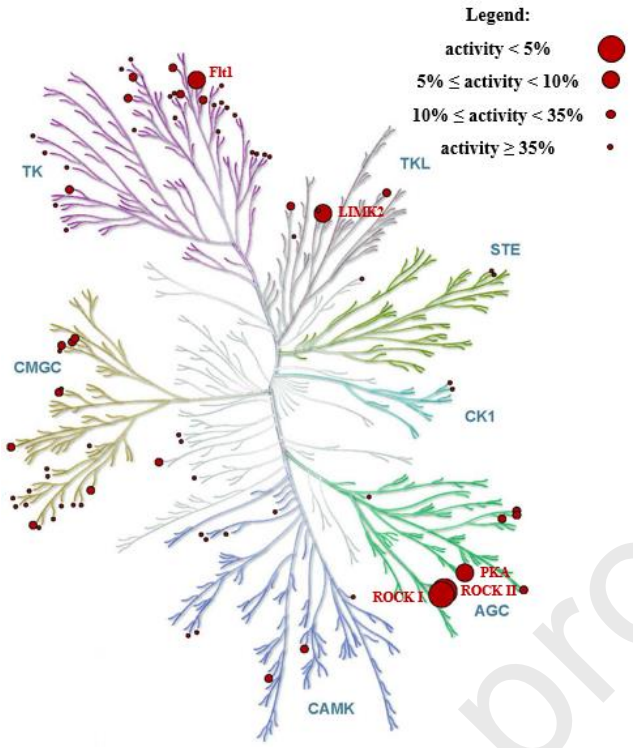

Figure 6. Kinase selectivity of **8k** shown on the human kinome dendrogram determined by the Kinase Profiler of Eurofins.

Collectively, we obtained a new series of thieno[2,3-*d*]pyrimidin-4(3*H*)-one derivatives as ROCK inhibitors. The most potent compound corresponds to **8k**, which showed IC_{50} values of 0.004 μM and 0.001 μM against ROCK I and ROCK II, respectively. *In vitro*, **8k** could efficiently inhibit ROCK activity in intact cells, alter cell morphology, and inhibit cell migration. **8k** could be a promising lead compound for drug discovery targeting ROCK and deserves further studies.

Acknowledgment

This work was supported by the National Natural Science Foundation of China (81773633, 21772130, and 81930125), National Science and Technology Major Project

(2018ZX09711002-014-002, 2018ZX09711002-011-019, 2018ZX09201018, 2018ZX09711003-003-006, and 2019ZX09301-135), and 1.3.5 project for disciplines of excellence, West China Hospital, Sichuan University.

Supporting Information

Supplementary data associated with this article can be found in the online version.

Reference

(1) Riento, K.; Ridley, A. J. *Nature Reviews Molecular Cell Biology* **2003**, *4*, 446.

(2) Guerra, F. S.; de Oliveira, R. G.; Manssour Fraga, C. A.; Mermelstein, C. d. S.; Fernandes, P. D. *Scientific Reports* **2017**, *7*, 1.

(3) Dayal, N.; Mikek, C. G.; Hernandez, D.; Naclerio, G. A.; Chu, E. F. Y.; Carter-Cooper, B. A.; Lapidus, R. G.; Sintim, H. O. *European Journal of Medicinal Chemistry* **2019**, *180*, 449.

(4) Hatzimouratidis, K.; Hatzichristiou, D. G. *Drugs* **2008**, *68*, 231.

(5) Wang, J.; Liu, X.; Zhong, Y. *International Journal of Oncology* **2013**, *43*, 1357.

(6) Sturdivant, J. M.; Royalty, S. M.; Lin, C.-W.; Moore, L. A.; Yingling, J. D.; Laethem, C. L.; Sherman, B.; Heintzelman, G. R.; Kopczynski, C. C.; deLong, M. A. *Bioorganic & Medicinal Chemistry Letters* **2016**, *26*, 2475.

(7) Shaw, D.; Hollingworth, G.; Soldermann, N.; Sprague, E.; Schuler, W.; Vangrevelinghe, E.; Duggan, N.; Thomas, M.; Kosaka, T.; Waters, N.; van Eis, M. J. *Bioorganic & Medicinal Chemistry Letters* **2014**, *24*, 4812.

(8) Satoh, K.; Fukumoto, Y.; Shimokawa, H. *American Journal of Physiology-Heart and Circulatory Physiology* **2011**, *301*, 287.

(9) Ho, K.-K.; Beasley, J. R.; Belanger, L.; Black, D.; Chan, J.-H.; Dunn, D.; Hu, B.; Klon, A.; Kultgen, S. G.; Ohlmeyer, M.; Parlato, S. M.; Ray, P. C.; Pham, Q.; Rong, Y.; Roughton, A. L.; Walker, T. L.; Wright, J.; Xu, K.; Xu, Y.; Zhang, L.; Webb, M. *Bioorganic & Medicinal Chemistry Letters* **2009**, *19*, 6027.

(10) Mueller, B. K.; Mack, H.; Teusch, N. *Nature Reviews Drug Discovery* **2005**, *4*, 387.

(11) Kuemper, S.; Mardakheh, F. K.; McCarthy, A.; Yeo, M.; Stamp, G. W.; Paul, A.; Worboys, J.; Sadok, A.; Jorgensen, C.; Guichard, S.; Marshall, C. J. *Elife* **2016**, *5*, 1.

(12) Kinoshita, S.; Koizumi, N.; Ueno, M.; Okumura, N.; Imai, K.; Tanaka, H.; Yamamoto, Y.; Nakamura, T.; Inatomi, T.; Bush, J.; Toda, M.; Hagiya, M.; Yokota, I.; Teramukai, S.; Sotozono, C.; Hamuro, J. *New England Journal of Medicine* **2018**, *378*, 995.

(13) Feng, Y.; LoGrasso, P. V.; Defert, O.; Li, R. *Journal of Medicinal Chemistry* **2016**, *59*, 2269.

(14) Inoue, T.; Tanihara, H. *Expert Opinion on Pharmacotherapy* **2017**, *18*, 1669.

(15) Hoy, S. M. *Drugs* **2018**, *78*, 389.

(16) Kimura, K.; Ito, M.; Amano, M.; Chihara, K.; Fukata, Y.; Nakafuku, M.; Yamamori, B.; Feng, J. H.; Nakano, T.; Okawa, K.; Iwamatsu, A.; Kaibuchi, K. *Science* **1996**, *273*, 245.

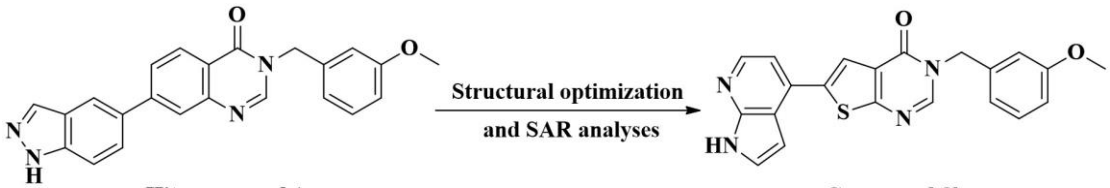

Hit compound 1
ROCK I IC_{50}: 3.106 μM
ROCK II IC_{50}: 0.088 μM

Compound 8k
ROCK I IC_{50}: 0.004 μM
ROCK II IC_{50}: 0.001 μM